

Solvation Dynamics in Nonaqueous Reverse Micelles

Hideaki Shirota* and Kazuyuki Horie*

Department of Chemistry and Biotechnology, Graduate School of Engineering, University of Tokyo,
7-3-1 Hongo, Bunkyo-ku, Tokyo 113-8656, Japan

Received: September 3, 1998; In Final Form: December 31, 1998

We have investigated the solvation dynamics of methanol and acetonitrile in reverse micelles for the first time. The solvation dynamics of both methanol and acetonitrile in reverse micelles show nonexponential features and unusual slow solvation components (from a few hundreds of picosecond to several nanoseconds). Interestingly, the solvation dynamics of methanol in reverse micelles becomes faster with a larger ratio of polar solvent to surfactant ($w = [\text{polar solvent}]/[\text{Aerosol OT}]$) of micelles. However, the w dependence of the solvation dynamics of acetonitrile in reverse micelles is not observed. The different w dependence of solvation dynamics in methanol and acetonitrile within reverse micelles should be arising from the presence of the intermolecular hydrogen-bonding network.

1. Introduction

Many chemical reactions, such as electron transfer, charge separation, and proton transfer, occur with substantial charge redistribution within the reactants. In polar solvents, such reactions are affected by the resulting changes in the solute–solvent interaction energy. The solvent relaxation time in response to the change in the solute charge distribution strongly affects the reaction dynamics. Studies of solvation dynamics are thus very important for a detailed understanding of the reaction dynamics in solution.^{1–9}

The solvent relaxation time can be measured by monitoring the time-dependent fluorescence Stokes shift after a probe molecule has been electronically excited. The spectral shift correlation function, $C(t)$, is given by

$$C(t) = \frac{\nu(t) - \nu(\infty)}{\nu(0) - \nu(\infty)} \quad (1)$$

where $\nu(t)$, $\nu(0)$, and $\nu(\infty)$ are the frequencies of fluorescence maximum at times t , 0, and ∞ , respectively. Namely, $t = 0$ is the time at which the electronic excitation occurs and $t = \infty$ corresponds to the time when the equilibrium of the orientation of the solvent molecules with the excited-state molecule has been reached.

Recent progress of laser technologies has made it possible to measure $C(t)$ of pure solvents at room temperature. Barbara and co-workers studied the solvation dynamics of a variety of liquids by using several probe molecules with the fluorescence up-conversion technique.^{4,10–13} The observed solvation dynamics were reasonably explained by the continuum solvation models. Maroncelli and co-workers measured the complete solvation dynamics including the inertial solvation component of various (polar and less polar) solvents by using a coumarin dye with a better time resolution system.^{14–18}

Recently, the solvation dynamics of solvents in special environments were investigated.^{19–34} Especially the solvation dynamics of water in micelles have been paid great attentions because it is one of the most simple models of biological systems. Lundgren et al. studied the solvation dynamics in bovine and human serum albumin sequestered within reverse

micelles.²³ The solvation dynamics of water in several sizes of Aerosol OT (AOT) reverse micelles were investigated by Zhang and Bright²⁴ and Bhattacharyya and co-workers.^{25,26} The extremely slow (nanosecond time scale) solvation processes were also observed in the reverse micelle systems, and the solvation dynamics of water depended strongly on the size of the micelles. Bhattacharyya and co-workers also studied the solvation dynamics of water in the Stern layer of micelles and showed that the solvation dynamics of water in ionic micelles and neutral micelles are quite different.²⁷ Levinger and co-workers studied the ultrafast solvation dynamics (a few hundreds of femtoseconds to several picoseconds) of water in AOT and lecithin reverse micelles by the femtosecond up-conversion technique.^{28–30} In contrast to the slow dynamics, the fast dynamics of reverse micelles was not strongly affected by the size of the micelles. They also studied the ultrafast solvation dynamics of a nonaqueous polar solvent (formamide) in reverse micelles for the first time.³¹

The reverse micelles are worthy of notice not only in simple biological models but also as microreactors. For many chemical reactions, water is not chosen as the solvent. Some cases were reported where nonaqueous reverse microemulsions were used as microreactors.³⁵ However, the studies of both the static and dynamic characteristics of nonaqueous reverse micelles are not that extensive in comparison with aqueous reverse micelles. In this work, we have investigated the solvation dynamics of methanol and acetonitrile in reverse micelles using a coumarin dye for the first time. Our main focusing points are as follows: (i) comparison of the solvation dynamics in pure solution and in reverse micelles; (ii) dependence of the solvation dynamics on the polar solvent content; (iii) comparison of the solvation dynamics of hydrogen-bonding liquid and aprotic liquid in reverse micelles.

2. Experimental Section

2.1. Sample Preparation. Laser-grade coumarin 343 (C343, Figure 1) was purchased from Exiton and used without further purification. Spectra-grade methanol (Nacalai Tesque), acetonitrile (Wako Pure Chemical), and cyclohexane (Wako Pure

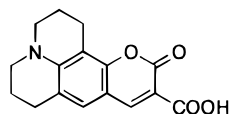


Figure 1. Structure of the probe molecule (coumarin 343) used in the present study.

Chemical) were also used as received. AOT (Wako Pure Chemical) was purified by the standard procedure.³⁶ Briefly, AOT was dissolved in methanol, into which hexane was added. After the mixture was shaken, the hexane phase was separated and the methanol phase was shaken three times with hexane. The methanol phase was evaporated, and the residue was dissolved in benzene and mixed with water. The benzene phase was separated after shaking, and the benzene phase was shaken two times with water. After being washed with water, the benzene phase was evaporated, and then the residue was dissolved in benzene. The benzene solution was azeotropically distilled three times to remove water. The AOT purified was dried at 393 K under vacuum for more than 12 h. Spectra-grade heptane (Wako Pure Chemical) was distilled with sodium before measurement. The concentration of the dye was around 10^{-5} M. The concentration of AOT was kept at 0.09 M. The amount of the polar solvent was kept at each value of the ratio of the polar solvent to the surfactant, $w = [\text{polar solvent}]/[\text{AOT}]$. The transparent sample solutions were obtained after sonication. The sizes of the micelles were estimated by dynamic light scattering measurements (Otsuka Electronics, ELS-400S). The diameters of the micelles were 2–4 nm.³⁷ These values are quite similar to the sizes of nonaqueous reverse micelles reported by Riter et al.³⁸

2.2. Time-Resolved Fluorescence Measurements. An optical parametric generator (EKSPLA, PG-401VIR) pumped by the third harmonic light of a mode-locked Nd:YAG laser (EKSPLA, PL2143B) was used as the light source. The excitation wavelength was adjusted to the absorption maximum wavelength (S_0 – S_1) of the sample. The power was about 1 mJ per pulse, and the repetition rate was 10 Hz. The fluorescence from the sample was passed through a polarizer set at the magic, perpendicular, or horizontal angle to the polarization of the pump light and a polychromator (JASCO, CT-25TP) and was detected by a streak camera (Hamamatsu, C4334–01). The fluorescence of the samples was detected by the different full time scales (1 ns and 10 ns). The fwhms of the instrument responses were 50–70 ps for the 1 ns full scale (solvation studies) and 170 ps for the 10 ns full scale (anisotropy studies). The optical path length of the sample was 5 mm. All the measurements were carried out at ambient temperature (295 ± 1 K).

Steady-state absorption and fluorescence spectra of C343 in reverse micelles were measured with a JASCO V-570 UV/VIS/NIR spectrophotometer and a Hitachi 850 fluorescence spectrophotometer before the dynamic measurements. The steady-state measurements were made at room temperature (295 ± 2 K).

3. Results

3.1. Steady-State Absorption and Fluorescence Spectra.

Figure 2 shows the steady-state absorption and fluorescence spectra of C343 in methanol/AOT/heptane micelles (solid line is for $w = 2$, dotted line is for $w = 4$, and broken line is for $w = 8$) (a) and acetonitrile/AOT/heptane micelles (solid line is for $w = 2$ and dotted line is for $w = 4$) (b). It is clear from the figure that both the absorption and fluorescence maxima of C343

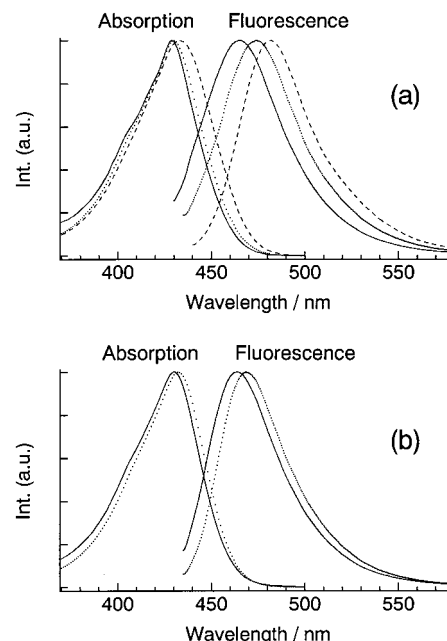


Figure 2. Steady-state absorption and fluorescence spectra of C343 in methanol/AOT/heptane micelles (a) and acetonitrile/AOT/heptane micelles (b). Solid lines are for $w = 2$, dotted lines are for $w = 4$, and broken lines are for $w = 8$.

TABLE 1: Steady-State Absorption and Fluorescence Maxima of C343 in Reverse Micelles and Pure Solvents

(a) Reverse Micelles			
polar solvent	w^a	$\lambda_{\text{abs}}/\text{nm}$	$\lambda_{\text{fl}}/\text{nm}$
methanol	2	429.1	464.1
methanol	4	430.2	473.8
methanol	8	433.0	481.7
acetonitrile	2	429.8	464.0
acetonitrile	4	432.2	468.5
(b) Pure Solvents			
solvent		$\lambda_{\text{abs}}/\text{nm}$	$\lambda_{\text{fl}}/\text{nm}$
methanol		443.9	491.3
acetonitrile		448.8	488.4
cyclohexane		428.8	435.7

^a $w = [\text{polar solvent}]/[\text{AOT}]$.

in larger w micelles shift to the longer wavelength. Especially the fluorescence maximum changes dramatically. The absorption and fluorescence maxima of C343 in reverse micelles measured are listed in Table 1 (a). For the comparison with those in homogeneous phases, the steady-state absorption and fluorescence spectra of C343 in pure methanol (line), acetonitrile (dots) (a), and cyclohexane (b) are shown in Figure 3. The absorption and fluorescence maxima of C343 in the pure solvents are also listed in Table 1 (b).

3.2. Dynamic Fluorescence Stokes Shift. Figure 4 shows typical examples of the time-resolved fluorescence spectra of C343 in acetonitrile/AOT/heptane micelles ($w = 4$). The spike at 432 nm of the time-resolved fluorescence spectrum ($t = 0$) is the excitation light. It is clear from the figure that the fluorescence maximum shifts to the longer wavelength as time progresses (line, 0 ns; dots, 0.3 ns; broken line, 0.9 ns; circles, 2.0 ns; triangles, 5.0 ns). Any dynamic fluorescence shifts of C343 in pure methanol and acetonitrile were not observed in the present experimental setup. To estimate the fluorescence maximum at each time, the fluorescence spectra measured are

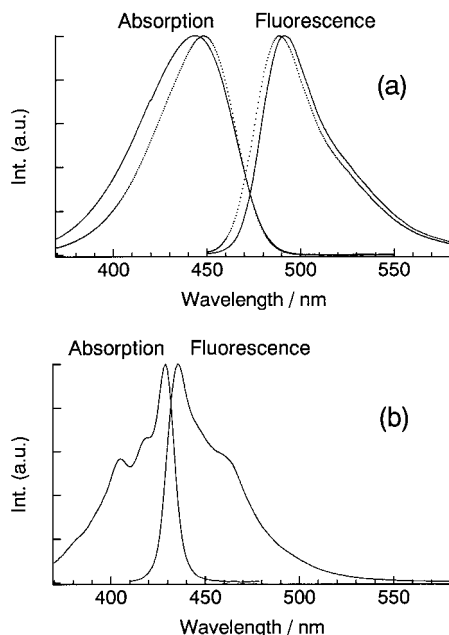


Figure 3. Steady-state absorption and fluorescence spectra of C343 in methanol (solid lines), acetonitrile (dotted lines) (a), and cyclohexane (b).

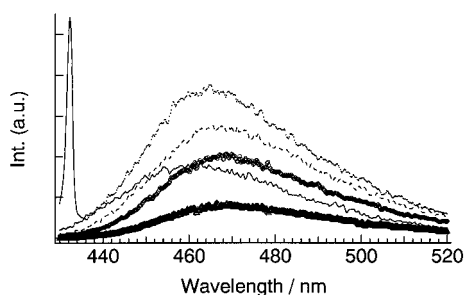


Figure 4. Time-resolved fluorescence spectra of C343 in acetonitrile/AOT/heptane micelles ($w = 4$). The spike at 432 nm of $t = 0$ spectrum is a laser pulse. The fluorescence maximum shifts as time progresses (line, 0 ns; dots, 0.3 ns; broken line, 0.9 ns; circles, 2.0 ns; triangles, 5.0 ns).

fitted with a log-normal line shape function³⁹

$$g(\nu) = g_0 \exp \left[-\ln(2) \left(\frac{\ln[1 + 2b(\nu - \nu_p)/\Delta]}{b} \right)^2 \right] \quad (2)$$

where g_0 , ν_p , b , and Δ are the peak height, peak frequency, asymmetric parameter, and width parameter, respectively. When $2b(\nu - \nu_p)/\Delta$ is less than -1 , $g(\nu)$ is taken as 0.

The characteristics of the solvation dynamics in reverse micelles are estimated by using eq 1. The $\nu(0)$ is defined as the frequency of the fluorescence maximum at the time of excitation by a laser pulse. The $\nu(\infty)$ is tentatively estimated from the extrapolation to the value for $C(\infty) = 0$ by fitting the experimental data to a biexponential function, because the slower component of solvation time (τ_{s2}) is larger than the fluorescence lifetime of C343 (around a few nanoseconds). Figure 5 shows the decay of $C(t)$ for C343 in methanol/AOT/heptane micelles (a) and in acetonitrile/AOT/heptane micelles (b). Circles, triangles, and squares represent $w = 2, 4$, and 8 , respectively. Because all the decays are not fitted by an exponential function, they are tentatively fitted with a biexponential function ($a_{s1} \exp(-t/\tau_{s1}) + a_{s2} \exp(-t/\tau_{s2})$). In the fitting equation, τ_{s1} and τ_{s2} are the two solvation times and a_{s1} and a_{s2} are the relative amplitudes of the two solvation components. The amplitudes are normalized

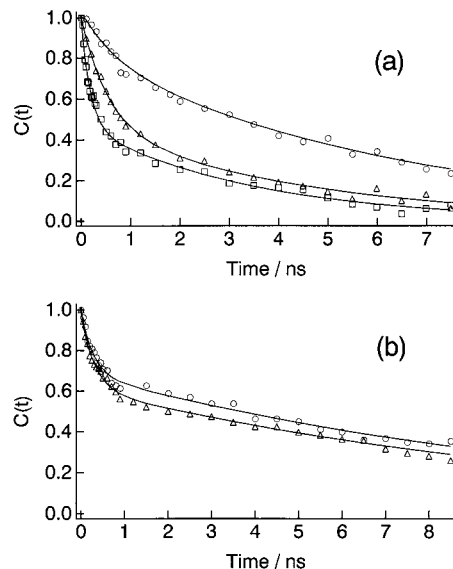


Figure 5. Spectral shift correlation function, $C(t)$, of C343 in methanol/AOT/heptane micelles (a) and acetonitrile/AOT/heptane micelles (b). Circles are for $w = 2$, triangles are for $w = 4$, and squares are for $w = 8$. The fitting curves analyzed are also shown (lines).

TABLE 2: Solvation Parameters for Methanol and Acetonitrile in Reverse Micelles

polar solvent	w^a	a_{s1}^b	τ_{s1}^b/ns	a_{s2}^b	τ_{s2}^b/ns	$\langle \tau_s \rangle^c/\text{ns}$
methanol	2	0.21	0.67	0.79	6.49	5.27
methanol	4	0.52	0.54	0.48	4.50	2.44
methanol	8	0.54	0.19	0.46	3.36	1.65
acetonitrile	2	0.33	0.28	0.67	11.3	7.66
acetonitrile	4	0.38	0.31	0.62	11.3	7.01

^a $w = [\text{polar solvent}]/[\text{AOT}]$. ^b Experimental error is $\pm 15\%$. ^c $\langle \tau_s \rangle = a_{s1}\tau_{s1} + a_{s2}\tau_{s2}$; $a_{s1} + a_{s2} = 1$.

for simplicity; $a_{s1} + a_{s2} = 1$. The fitted curves are also shown in the figure (lines). The obtained solvation parameters are summarized in Table 2. The table also lists the average solvation time $\langle \tau_s \rangle$. The $\langle \tau_s \rangle$ is defined as

$$\langle \tau_s \rangle \equiv \int_0^\infty C(t) dt$$

$$= \int_0^\infty [a_{s1} \exp(-t/\tau_{s1}) + a_{s2} \exp(-t/\tau_{s2})] dt = a_{s1}\tau_{s1} + a_{s2}\tau_{s2} \quad (3)$$

The important points to be noted from Figure 5 and Table 2 are as follows. (i) The solvation times of methanol and acetonitrile in reverse micelles are extremely slow in comparison with those in pure methanol and acetonitrile. (ii) Both the fast and slow solvation times of methanol in reverse micelles depend strongly on the ratio, w , of the polar solvent to the surfactant, while the solvation times of acetonitrile in reverse micelles are insensitive to w .

3.3. Fluorescence Anisotropy. To investigate the location of the probe molecule in the micellar interior, the time-resolved fluorescence anisotropy of C343 in reverse micelles is measured. The anisotropy decay, $r(t)$, is given by

$$r(t) = \frac{I_{\parallel}(t) - I_{\perp}(t)}{I_{\parallel}(t) + 2I_{\perp}(t)} \quad (4)$$

where $I_{\parallel}(t)$ and $I_{\perp}(t)$ are tail-matched fluorescence decays polarized parallel and perpendicular to the polarization of the excitation light, respectively. Figure 6 shows the fluorescence

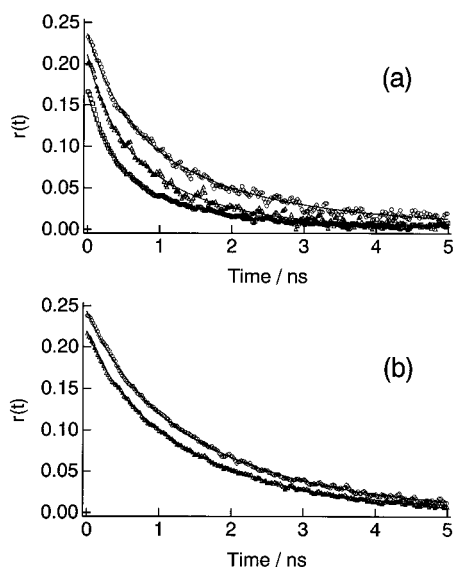


Figure 6. Fluorescence anisotropy decays in nonaqueous reverse micelles: (a) methanol/AOT/heptane micelles; (b) acetonitrile/AOT/heptane micelles. Circles are for $w = 2$, triangles are for $w = 4$, and squares are for $w = 8$. The fitting curves analyzed are also shown (lines).

TABLE 3: Parameters of Anisotropy Decays for Methanol and Acetonitrile in Reverse Micelles

polar solvent	w^a	a_{r1}^b	τ_{r1}^b/ns	a_{r2}^b	τ_{r2}^b/ns	$r(0)$
methanol	2	0.09	0.44	0.15	1.65	0.24
methanol	4	0.06	0.26	0.14	1.13	0.20
methanol	8	0.06	0.25	0.11	0.97	0.17
acetonitrile	2	0.05	0.45	0.21	1.77	0.26
acetonitrile	4	0.04	0.42	0.20	1.49	0.24

^a $w = [\text{polar solvent}]/[\text{AOT}]$. ^b Experimental error is $\pm 10\%$.

anisotropy decays of C343 in methanol/AOT/heptane micelles (a) and in acetonitrile/AOT/heptane micelles (b) (circles are for $w = 2$, triangles are for $w = 4$, and squares are for $w = 8$). All the decays are tentatively fitted by a biexponential function ($a_{r1} \exp(-t/\tau_{r1}) + a_{r2} \exp(-t/\tau_{r2})$), and the fitted curves are also shown in Figure 6 (lines). The anisotropy parameters obtained are summarized in Table 3. The initial anisotropy ($r(0)$) is also listed in the table. The reason that $r(0)$ is smaller than 0.4 would be due to the contribution of C343 in the middle of the micelle pool and/or in bulk (heptane) medium, because the anisotropy decays in pure methanol and acetonitrile were not observed in the present laser system. From the comparison with the anisotropy decay times of pure methanol and acetonitrile (methanol, 5.9 and 44 ps; acetonitrile, 22 ps⁴⁰), the anisotropy decays in reverse micelles are rather slow. As shown in Figure 6 and Table 3, the rotational motion of C343 in the larger- w micelles is faster than that in the smaller- w micelles. This indicates that the restrictive environment in reverse micelles becomes looser with increasing w . A similar phenomenon was also observed in water/AOT reverse micelles.²⁸

4. Discussion

4.1. Solvation Dynamics in Reverse Micelles: Comparison with Solvation Dynamics in Pure Solvents. Let us compare the solvation dynamics in pure solvents and in reverse micelles. The time resolution using the present laser system is insufficient to resolve the solvation dynamics in pure solution. The solvation dynamics of pure methanol and acetonitrile, however, were measured by coumarins using better time resolution systems by several groups.^{12,13,16,18,40–45} The solvation dynamics of pure

methanol showed highly nonexponential features and occurred within the time scale in the range 1–10 ps (average solvation time after removing the inertial component was around 6 ps).^{12,13,16,18,40–45} The solvation dynamics of pure acetonitrile is also extremely fast (< 1 ps).^{12,13,16,40,45} The solvation dynamics in methanol and acetonitrile within reverse micelles show also nonexponential features and around 1000 times slower than those in pure solvents. The nonexponential decay of the solvation dynamics in reverse micelles should not be arising from the contribution of solvation process of the pure solvent, because the fast solvation times in reverse micelles are not identical to the solvation times in pure solvents and also the dynamic fluorescence Stokes shifts in pure solvents were not observed in the present apparatus.

The solvation dynamics in aqueous reverse micelles show also a nonexponential feature.^{25,26,28,29} This is due to the environmentally different solvent molecules in reverse micelles. In biological systems, the water is believed to consist of two kinds of water molecules, namely, bound and free water molecules.⁴⁶ The bound water molecule shows very slow relaxation arising from the strong interaction between the biomolecule and water molecule. The nonaqueous polar solvent in reverse micelle systems would also consist of some different kinds of molecules. As shown in Figure 6 and Table 3, the rotational diffusions of C343 in acetonitrile/AOT/heptane and methanol/AOT/heptane reverse micelles show the nonexponential feature and the rather slow component in comparison with those of coumarin 153 in pure solvents.⁴⁰ The result indicates that the C343 in reverse micelles position in several different environments. The solvation dynamics of methanol and acetonitrile in reverse micelles should thus show the nonexponential features and the unusual slow dynamics.⁴⁷

On the other hand, we should consider the effect of the sodium cation of AOT. The effect of the presence of an ion on the solvation dynamics in solution has been investigated experimentally and theoretically.^{28,48–54} They suggested that the slow component of the solvation dynamics appeared due to the presence of the ion. Riter et al. studied the effect of the counterion of AOT on the solvation dynamics of water in AOT reverse micelles.³⁰ They showed slower solvation dynamics in the sodium cation micelles than in the ammonium cation micelles and concluded that the immobilization of water in AOT reverse micelles arises largely from the interaction of the water with a high concentration of sodium cations present in the micellar interior. The hydrogen-bonding liquid molecules in contact with AOT showed unusual hydrogen-bonding interactions.^{55–59} By IR measurement, Christopher et al.⁵⁸ and Moran et al.⁵⁹ showed that three or four water molecules bridge between the sulfonate and sodium ions in AOT reverse micelles. Namely, these water molecules strongly bind to the wall of the reverse micelles through the sodium cations. The microscopic picture of methanol/AOT/heptane micelles should be similar to that of aqueous reverse micelles, because some methanol molecules bridge between the sulfonate and sodium ions due to the presence of hydroxyl groups. In the case of acetonitrile, the slow component (several nanoseconds) of the solvation dynamics was observed in the presence of a salt by several groups.^{49–51} Since an AOT molecule has a sodium cation, the solvation dynamics in acetonitrile/AOT/heptane micelles should become slow even in the absence of the hydrogen-bonding network between water molecules and sodium and sulfonate ions. The effect of salt on the solvation dynamics will be further discussed in a later section.

The estimation of the real time-zero fluorescence spectra of

TABLE 4: Calculated Time-Zero Fluorescence Maxima $\lambda_{\text{cal}}(0)$, Observed Time-Zero Fluorescence Maxima $\lambda(0)$, Time-Infinity Fluorescence Maxima $\lambda(\infty)$, and Missing Components of C343 in Reverse Micelles

polar solvent	w^a	$\lambda_{\text{cal}}(0)/\text{nm}$	$\lambda(0)/\text{nm}$	$\lambda(\infty)/\text{nm}$	missing component ^c
methanol	2	451.4	452.9	476.2	0.06
methanol	4	452.7	458.1	479.9	0.21
methanol	8	455.8	464.6	483.9	0.33
acetonitrile	2	450.4	455.1	470.9	0.24
acetonitrile	4	452.0	460.9	475.5	0.39

^a $w = [\text{polar solvent}]/[\text{AOT}]$. ^b Estimated from eq 5. ^c Calculated as $(\nu_{\text{cal}}(0) - \nu(0))/(\nu_{\text{cal}}(0) - \nu(\infty))$.

C343 in reverse micelles may give us important information: What percentage of the solvation process can we observe? The time-zero spectrum here means a fluorescence spectrum without any solvent relaxation. It is not the experimental time-zero spectrum (because the response of our laser system has a fwhm of 50–70 ps). We estimate the time-zero spectra of C343 in reverse micelles by using the method proposed by Fee and Maroncelli.⁶⁰ The time-zero frequency can be estimated from the steady-state absorption and fluorescence spectra.

$$\nu_{\text{p,md}}(t=0) \approx \nu_{\text{p,md}}(\text{abs}) - [\nu_{\text{np,md}}(\text{abs}) - \nu_{\text{np,md}}(\text{fl})] \quad (5)$$

where the subscripts “p” and “np” refer to the polar and nonpolar spectra, respectively, and the frequencies here are not the values at maxima but correspond to the midpoint frequencies, ν_{md} , in the solvents. The midpoint frequency is given by

$$\nu_{\text{md}} = (\nu_- + \nu_+)/2 \quad (6)$$

where ν_- and ν_+ are the low and high frequencies on the half-height points of the spectrum. Cyclohexane is used as the nonpolar solvent in the present work. The maximum frequency at time zero, $\nu_{\text{p}}(t=0)$, is estimated as the sum of $\nu_{\text{p,md}}(t=0)$ and the difference between the midpoint and maximum frequencies in the steady-state fluorescence spectrum of the same system. The time-zero maximums wavelength calculated from eq 6, $\lambda_{\text{cal}}(0) = 1/\nu_{\text{p}}(t=0)$, in micelles are listed in Table 4. The observed time-zero wavelength, $\lambda(0) = 1/\nu(0)$, the wavelength at infinite time, $\lambda(\infty) = 1/\nu(\infty)$, and the proportions of missing component $((\nu_{\text{cal}}(0) - \nu(0))/(\nu_{\text{cal}}(0) - \nu(\infty)))$ are also listed in the table.

The missing component corresponding to the unobservable solvation component for the present time resolution system increases with the increase in the ratio w . The tendency seems to be reasonable because the property of the polar solvent in reverse micelles with larger w becomes similar to that of the pure solvent for the larger content of polar solvent in reverse micelles. This is consistent with the results of both the steady-state absorption and fluorescence measurements. The steady-state absorption and fluorescence maxima of C343 in reverse micelles are shifted with the increase in w in the direction toward those in the pure solvents (Table 1). The rotational diffusion of C343 in reverse micelles shows also such a feature, namely, the difference of the value of $r(0)$ from 0.4 becomes larger with larger- w micelles (Figure 6 and Table 3).

4.2. Dependence of Solvation Dynamics on the Ratio of Polar Solvent to Surfactant, w . The most astonishing point in the present results is the w dependence of the solvation dynamics of methanol and acetonitrile in reverse micelles. It is clear from Figure 5 and Table 2 that the features of the w dependence of the solvation dynamics in methanol and acetonitrile within reverse micelles are rather different. Both the fast and slow

solvation times of methanol in reverse micelles become smaller with larger- w micelles (τ_{s1} : 0.67 ns ($w=2$), 0.54 ns ($w=4$), 0.19 ns ($w=8$). τ_{s2} : 6.49 ns ($w=2$), 4.50 ns ($w=4$) 3.36 ns ($w=8$)). In contrast to the tendency of methanol, the w dependence of the solvation dynamics of acetonitrile in reverse micelles is not observed within experimental accuracy (τ_{s1} : 0.28 ns ($w=2$), 0.31 ns ($w=4$). τ_{s2} : 11.3 ns ($w=2$), 11.3 ns ($w=4$)).

The comparison of the present results with those of water/AOT/heptane micelles may give us some valuable information. Sarkar et al. investigated the solvation dynamics in water/AOT/heptane micelles and observed the large w dependence of solvation dynamics (8.0 ns for $w=4$ and 1.7 ns for $w=32$).²⁵ Since the viscosity and dielectric constant of water in reverse micelles are strongly influenced by w ,^{61–64} the solvation time should change. In the case of a single Debye-type solvent, a single-exponential function is predicted for $C(t)$ within a context of a continuum model with a single solvation time

$$\tau_{\text{s}} \approx \tau_{\text{L}} \approx (\epsilon_{\infty}/\epsilon_0)\tau_{\text{D}} \quad (7)$$

where τ_{L} is the longitudinal relaxation time, ϵ_{∞} is the infinite-frequency dielectric constant, and ϵ_0 is the static dielectric constant. τ_{D} is the Debye relaxation time, which is approximately proportional to the relaxation time of the single-molecule dipole, τ_1 .⁶⁵ In dipole liquids, τ_1 is given by

$$\tau_1 = \frac{4\pi\eta a^3}{k_{\text{B}}T} \quad (8)$$

where η is the viscosity, a is the radius of molecule, k_{B} is the Boltzmann constant, and T is the absolute temperature.⁶⁶ From the measurements of the rotational diffusion of the fluorescent molecule in different- w micelles, it is known that the rotational diffusion coefficient becomes smaller with smaller ratio w of micelles.⁶² Since the viscosity of water in reverse micelles is higher with smaller- w micelles, the solvation time should be larger.

The solvation dynamics of acetonitrile in reverse micelles, however, is not affected by the change in the ratio w . This difference between methanol and acetonitrile might be due to the existence of a hydrogen-bonding network. Das et al. compared the solvation dynamics of water and heavy water in reverse micelles.²⁶ The solvation time of heavy water in reverse micelles is larger than that of water in reverse micelles ($\langle\tau_{\text{s}}\rangle(\text{D}_2\text{O})/\langle\tau_{\text{s}}\rangle(\text{H}_2\text{O}) = 1.2$). The deuterium isotope effects on the solvation dynamics of pure hydrogen-bonding liquids (methanol and anilines) come mainly from the difference in the stabilization energies of the intermolecular hydrogen bonds in normal and deuterated liquids.^{43,67,68} Since methanol can form a hydrogen-bonding network, the slow solvation dynamics (several hundred picoseconds to nanoseconds) of methanol in reverse micelles could be strongly influenced by the hydrogen-bonding interactions in the same manner as that of water in reverse micelles. As a result of the hydrogen-bonding interactions, the solvent molecules near the ionic headgroup of the surfactant and those in the position apart from the surfactant interact strongly with each other.

In contrast to hydrogen-bonding liquids, acetonitrile molecules give the dipole–dipole interaction that is weaker than the hydrogen-bonding interaction. The viscosity of neat methanol is 0.544 cP at 298 K, while the viscosity of neat acetonitrile is 0.369 cP at 298 K.⁶⁹ The interactions between acetonitrile molecules that are in different environments (near and apart from surfactants), thus, should be weaker than those between

methanol molecules in different environments. Accordingly, the solvation times of acetonitrile in different- w micelles show the same time constants but the extent of the missing component is larger with larger- w micelles. The different features of the w dependence of the solvation dynamics in methanol and acetonitrile within reverse micelles, thus, should originate from the different interactions. The interaction of solvent molecules near the surfactant wall is very strong, and the interaction strength becomes weaker with being apart from the wall. The interaction strength dependence of w in methanol micelles should be arising from the hydrogen-bonding network. No w dependence of the solvation dynamics in acetonitrile micelles might be due to the weak intermolecular interaction.

Another possible explanation for this different w dependence of the solvation dynamics in methanol/AOT/heptane and acetonitrile/AOT/heptane micelles is that the counterions of the surfactant (sodium cation) in methanol and acetonitrile contribute differently to the solvation dynamics. As mentioned above, some methanol molecules should bridge between the sulfonate and sodium ions as water molecules do. In contrast to methanol molecules, acetonitrile molecules in reverse micelles could not bridge between the sulfonate and sodium ions in AOT reverse micelles due to the lack of the source of the hydrogen bond.

The comparison of the solvation dynamics in reverse micelles with the solvation dynamics of ionic solutions may give us some information. The slow component of the solvation dynamics in ion solutions appears due to a sort of ion-probe association. Chapman and Maroncelli reported that the solvation dynamics of NaClO₄/acetonitrile solution is almost insensitive to the concentration of the salt in the high concentration region (>1.5 M).⁵¹ The concentration of the sodium cation is very high in the acetonitrile pool of the reverse micelles (~ 5 M for $w = 4$ and ~ 10 M for $w = 2$). Thus, no w dependence of the solvation dynamics in the acetonitrile/AOT/heptane micelles might be coming from the effect of the sodium cation. In contrast to the NaClO₄/acetonitrile solution, the nanosecond time scale solvation dynamics in a NaClO₄/methanol solution was not observed due to no ionic contribution. Such a difference of the effect of ions on the solvation dynamics in ionic acetonitrile and methanol solutions might affect the solvation dynamics in nonaqueous reverse micelles.

5. Conclusion

We have investigated the solvation dynamics of nonaqueous polar solvents (methanol and acetonitrile) in reverse micelles for the first time. The solvation dynamics of the solvents in reverse micelles are about 10^3 times slower than those of the pure solvents. The solvation dynamics in reverse micelles show the nonexponential features. The solvation dynamics of methanol in reverse micelles depends strongly on the ratio w of micelles. The solvation dynamics of acetonitrile in reverse micelles, however, is independent of the ratio w . The different features of the solvation dynamics would be attributed to the role of the hydrogen bonds in methanol and its absence in acetonitrile.

Acknowledgment. We are grateful to Prof. Takehiko Kitamori, Mr. Hiroharu Yui, and Mr. Yoshinori Yoneda (University of Tokyo) for their kind help in preparing the picosecond laser system. We are also grateful to Prof. Kohzo Ito, Mr. Takeshi Shimomura, and Mr. Shinpei Tanaka (University of Tokyo) for their kind help in dynamic light scattering measurements. This work is partly supported by a Grant-in-Aid for Scientific Research on Priority Areas, "New Polymers

and Their Nano-Organized Systems" (No. 277/0923211), from the Ministry of Education, Science, Sports and Culture of Japan.

References and Notes

- (1) Frauenfelder, H.; Wolynes, P. G. *Science* **1985**, *229*, 337.
- (2) Maroncelli, M.; MacInnis, J.; Fleming, G. R. *Science* **1989**, *243*, 1674.
- (3) Bagchi, B. *Annu. Rev. Phys. Chem.* **1989**, *40*, 115.
- (4) Barbara, P. F.; Jarzeba, W. *Adv. Photochem.* **1990**, *15*, 1.
- (5) Weaver, M. J.; McManis, G. E., III *Acc. Chem. Res.* **1990**, *23*, 294.
- (6) Barbara, P. F.; Walker, G. C.; Smith, T. P. *Science* **1992**, *256*, 975.
- (7) Heitele, H. *Angew. Chem., Int. Ed. Engl.* **1993**, *32*, 359.
- (8) Yoshihara, K.; Tominaga, K.; Nagasawa, Y. *Bull. Chem. Soc. Jpn.* **1995**, *68*, 696.
- (9) Maroncelli, M. *J. Mol. Liq.* **1993**, *57*, 1.
- (10) Nagarajan, V.; Brearley, A. M.; Kang, T. J.; Barbara, P. F. *J. Chem. Phys.* **1987**, *86*, 3183.
- (11) Kahlow, M. A.; Kang, T. J.; Barbara, P. F. *J. Chem. Phys.* **1988**, *88*, 2372.
- (12) Kahlow, M. A.; Jarzeba, W.; Kang, T. J.; Barbara, P. F. *J. Chem. Phys.* **1989**, *90*, 151.
- (13) Jarzeba, W.; Walker, G. C.; Johnson, A. E.; Barbara, P. F. *J. Chem. Phys.* **1989**, *152*, 57.
- (14) Jimenez, R.; Fleming, G. R.; Kumar, P. V.; Maroncelli, M. *Nature* **1994**, *369*, 471.
- (15) Chapman, C. F.; Fee, R. S.; Maroncelli, M. *J. Phys. Chem.* **1995**, *99*, 4811.
- (16) Horng, M. L.; Gardecki, J. A.; Papazyan, A.; Maroncelli, M. *J. Phys. Chem.* **1995**, *99*, 17311.
- (17) Reynolds, L.; Gardecki, J. A.; Frankland, S. J. V.; Horng, M. J.; Maroncelli, M. *J. Phys. Chem.* **1996**, *100*, 10337.
- (18) Rosenthal, S. J.; Jimenez, R.; Fleming, G. R.; Kumar, P. V.; Maroncelli, M. *J. Mol. Liq.* **1994**, *60*, 25.
- (19) Vajda, S.; Jimenez, R.; Rosenthal, S. J.; Fidler, V.; Fleming, G. R.; Castner, E. W., Jr. *J. Chem. Soc., Faraday Trans.* **1995**, *91*, 867.
- (20) Streck, C.; Mel'nikchenko, B.; Richert, R. *Phys. Rev. B* **1996**, *53*, 5341.
- (21) Yanagimachi, M.; Tamai, N.; Masuhara, H. *Chem. Phys. Lett.* **1992**, *200*, 469.
- (22) Datta, A.; Pal, S. K.; Mandal, D.; Bhattacharyya, K. *J. Phys. Chem. B* **1998**, *102*, 6114.
- (23) Lundgren, J. S.; Heitz, M. P.; Bright, F. V. *Anal. Chem.* **1995**, *67*, 3775.
- (24) Zhang, J.; Bright, F. V. *J. Phys. Chem.* **1991**, *95*, 7900.
- (25) Sarkar, N.; Das, K.; Datta, A.; Das, S.; Bhattacharyya, K. *J. Phys. Chem.* **1996**, *100*, 10523.
- (26) Das, S.; Datta, A.; Bhattacharyya, K. *J. Phys. Chem. A* **1997**, *101*, 3299.
- (27) Sarkar, N.; Datta, A.; Das, S.; Bhattacharyya, K. *J. Phys. Chem.* **1996**, *100*, 15483.
- (28) Riter, R. E.; Willard, D. M.; Levinger, N. E. *J. Phys. Chem. B* **1998**, *102*, 2705.
- (29) Willard, D. M.; Riter, R. E.; Levinger, N. E. *J. Am. Chem. Soc.* **1998**, *120*, 4151.
- (30) Riter, R. E.; Undiks, E. P.; Levinger, N. E. *J. Am. Chem. Soc.* **1998**, *120*, 6062.
- (31) Riter, R. E.; Undiks, E. P.; Kimmel, J. R.; Levinger, N. E. *J. Phys. Chem. B* **1998**, *102*, 7931.
- (32) Jordan, J. D.; Dunbar, R. A.; Bright, F. V. *Anal. Chem.* **1995**, *67*, 2436.
- (33) Datta, A.; Das, S.; Mandal, D.; Pal, S. K.; Bhattacharyya, K. *Langmuir* **1997**, *13*, 6922.
- (34) Nandi, N.; Bagchi, B. *J. Phys. Chem.* **1996**, *100*, 13914.
- (35) Samii, A. A.-Z.; de Saignac, A.; Rico, I.; Lattes, A. *Tetrahedron* **1985**, *41*, 3683.
- (36) Maitra, A. N.; Eicke, H.-F. *J. Phys. Chem.* **1981**, *85*, 2687.
- (37) For the small signals and the tiny sizes, the experimental error is quite large (± 2 nm). The diameters of the micelles are 2.6 nm for $w = 2$ (methanol), 2.4 nm for $w = 4$ (methanol), 3.0 nm for $w = 8$ (methanol), 2.6 nm for $w = 2$ (acetonitrile), and 3.8 nm for $w = 4$ (acetonitrile).
- (38) Riter, R. E.; Kimmel, J. R.; Undiks, E. P.; Levinger, N. E. *J. Phys. Chem. B* **1997**, *101*, 8292.
- (39) Siano, D. B.; Metzler, D. E. *J. Chem. Phys.* **1969**, *51*, 1856.
- (40) Horng, M.-L.; Gardecki, J. A.; Maroncelli, M. *J. Phys. Chem. A* **1997**, *101*, 1030.
- (41) Rosenthal, S. J.; Scherer, N. F.; Cho, M.; Xie, X.; Schmidt, M. E.; Fleming, G. R. *Ultrafast Phenomena VIII*; Springer-Verlag: Berlin, 1993; p 616.
- (42) Tominaga, K.; Walker, G. C. *J. Photochem. Photobiol. A: Chem.* **1995**, *87*, 127.

- (43) Shirota, H.; Pal, H.; Tominaga, K.; Yoshihara, K. *J. Phys. Chem.* **1996**, *100*, 14575.
- (44) Gustavsson, T.; Gulbinas, V.; Gurzadyan, G.; Mialocq, J.-C.; Pommeret, S.; Sorginus, M.; van der Meulen, P. *J. Phys. Chem. A* **1998**, *102*, 4229.
- (45) Rosenthal, S. J.; Xie, X.; Du, M.; Fleming, G. R. *J. Chem. Phys.* **1991**, *95*, 4715.
- (46) Nandi, N.; Bagchi, B. *J. Phys. Chem. B* **1997**, *101*, 10954 and references therein.
- (47) Riter et al. reported that methanol and acetonitrile dissolve in nonpolar solvents in ref 38. We are studying the dynamics in polar solvent/nonpolar solvent mixtures. The parallel and perpendicular detected fluorescence decays of C343 in near saturated methanol and acetonitrile/heptane mixtures are almost the same within experimental error. Interestingly, the dynamic fluorescence Stokes shifts in the methanol/heptane mixture are observed (~ 300 ps, no nanosecond component). However, no dynamic fluorescence Stokes shifts in the acetonitrile/heptane mixture are observed within experimental error. We thus conclude that the slow solvation dynamics in reverse micelles are not arising from the binary solution effect except for the hundreds of picosecond component in methanol/AOT/heptane micelles.
- (48) Huppert, D.; Ittah, V.; Kosower, E. M. *Chem. Phys. Lett.* **1989**, *159*, 267.
- (49) Ittah, V.; Huppert, D. *Chem. Phys. Lett.* **1990**, *173*, 496.
- (50) Bart, E.; Huppert, D. *Chem. Phys. Lett.* **1992**, *195*, 37.
- (51) Chapman, C. F.; Maroncelli, M. *J. Phys. Chem.* **1991**, *95*, 9095.
- (52) Guàrdia, E.; Padró, J. A. *J. Phys. Chem.* **1990**, *94*, 6049.
- (53) Chandra, A.; Patey, G. N. *J. Chem. Phys.* **1994**, *100*, 1552.
- (54) Neria, E.; Nitzan, A. *J. Chem. Phys.* **1994**, *100*, 3855.
- (55) Hauser, H.; Haering, G.; Pande, A.; Luisi, P. L. *J. Phys. Chem.* **1989**, *93*, 7869.
- (56) Onori, G.; Santucci, A. *J. Phys. Chem.* **1993**, *97*, 5430.
- (57) Karukstis, K. K.; Fraziner, A. A.; Martula, S.; Whiles, J. A. *J. Phys. Chem.* **1996**, *100*, 11133.
- (58) Christopher, D. J.; Yarwood, J.; Belton, P. S.; Hills, B. P. *J. Colloid Interface Sci.* **1992**, *152*, 465.
- (59) Moran, P. D.; Bowmaker, G. A.; Cooney, R. P.; Barlett, J. R.; Woolfrey, J. L. *Langmuir* **1995**, *11*, 738.
- (60) Fee, R. S.; Maroncelli, M. *Chem. Phys.* **1994**, *183*, 235.
- (61) Kondo, H.; Miwa, I.; Sunamoto, J. *J. Phys. Chem.* **1982**, *86*, 4826.
- (62) Zinsli, P. E. *J. Phys. Chem.* **1979**, *83*, 3223.
- (63) Belletête, M.; Lachapelle, M.; Durocher, G. *J. Phys. Chem.* **1990**, *94*, 5337.
- (64) Hasegawa, M.; Sugimura, T.; Suzaki, Y.; Shindo, Y.; Kitahara, A. *J. Phys. Chem.* **1994**, *98*, 2120.
- (65) Madden, P.; Kivelson, D. *Adv. Chem. Phys.* **1984**, *56*, 467.
- (66) Fröhlich, H. *Theory of Dielectrics*, 2nd ed.; Oxford Press: Oxford, 1958; Chapter 3.
- (67) Pal, H.; Nagasawa, Y.; Tominaga, K.; Kumazaki, S.; Yoshihara, K. *J. Chem. Phys.* **1995**, *102*, 7758.
- (68) Shirota, H.; Pal, H.; Tominaga, K.; Yoshihara, K. *J. Phys. Chem. A* **1998**, *102*, 3089.
- (69) *CRC Handbook of Chemistry and Physics*, 74th ed.; CRC Press: Boca Raton, 1993.